

Application Note AN-EC-041

# 采用EQCM-D与EC-Raman用技研究 程

## EQCM-D with 3T analytik & Metrohm Autolab

An Electrochemical Quartz Crystal Microbalance with Dissipation Monitoring (EQCM-D) is a powerful analytical device. In contrast to traditional EQCM, which only correlates the mass changes on the electrode with the electrochemical signal, EQCM-D also correlates the damping of the oscillation caused by the local environment. In air this effect is almost negligible, however when the crystal is

immersed in an electrolyte, energy transfers from the oscillating crystal to the local environment, and the resulting damping signal has diagnostic value. For example, it can give insight into the structure of electrodeposited layers, and how different conditions will affect the resulting layer. EQCM-D can be applied to many areas of electrochemistry, including corrosion and energy.

This Application Note describes the use of EQCM-D to study deposition of  $\text{Ni}(\text{OH})_2$ , which is used for Ni-MH batteries and in electrocatalysis for the activation of small molecules. The eSorptionProbe from 3T analytik is presented in a beaker setup as well as integrated into an electrochemistry Raman cell. By measuring

## SAMPLE AND EXPERIMENTAL DETAILS

The potentiostat/galvanostat used is a Metrohm Autolab AUT204 equipped with the FRA32M module. The EQCM-D system is a 3T analytik, eSorptionProbe OS. With this system, fundamental and several overtone frequencies can be measured. This Application Note focuses on the fundamental frequency.

The working electrode consists of a 10 MHz EQCM Au crystal (active area  $19.2 \text{ mm}^2$ ) encased in a plastic substrate, similar to a screen-printed electrode (see **Figure 1**). It can be mounted onto a probe, which can then be inserted into most standard electrochemical cells (CORR250.CELL.S is used here), provided a suitable aperture is available. Note that care should be taken to insert the probe slowly into the electrolyte, and to not immerse the electrical contact. The software packages used are NOVA, qGraph, and qGraph Viewer for associating the QCM-D and electrochemical data.

This experiment consists of three parts. The first is a galvanostatic deposition experiment whereby nickel is deposited on the gold crystal as  $\text{Ni}(\text{OH})_2$  and the second is a cyclic voltammetry (CV) experiment in which the

frequency and damping (dissipation) of the fundamental resonance and multiple harmonics, the eSorption Probe extends the analytical capabilities to study soft, viscoelastic layer deposition alongside electrochemical measurements.



**Figure 1.** The crystal Pre (bottom) and Post (top) deposition.

deposited layer is electrochemically cycled to simulate real-life charging/discharging of a battery. The parameters of each experiment are summarized in **Table 1**.

**Table 1.** Parameters used in part 1 and 2 of this experiment.

Component	Part 1	Part 2
Technique	Chronopotentiometry	Cyclic voltammetry
Parameters	100 $\mu$ A 300 seconds	Start/Stop: 0 V Upper: 0.9 V Lower: -0.2 V Scan rate: 0.01 V/s
Cell	Two-electrode	Three-electrode
Working electrode	QCM Au Crystal	QCM Au Crystal
Counter electrode	Pt sheet	Pt sheet
Reference electrode	-	Ag/AgCl
Electrolyte	50 mmol/L NiSO <sub>4</sub>	0.1 mol/L NaOH

In the first two experiments, the QCM-D data is recorded simultaneously with the electrochemical data. The data can be associated after the measurement with tools provided in the qGraph software.

In the third part, a second EQCM-D probe is inserted into an EC-Raman cell (DRP-RAMANCELL-M) and electrochemically roughened to produce a SERS substrate, after which the first two parts of the experiment are repeated combined with monitoring of the Raman spectra. Light-induced detuning (LID) impacts the simultaneous collection of EQCM and Raman data, so spectra are only collected pre and post cycling of the film between Ni(OH)<sub>2</sub>

and NiOOH which is more Raman active. There are strategies in the literature to overcome this effect, but these are not trialed here [1].

The parameters of the electrochemical roughening are summarized in **Table 2**. An i-Raman Plus 532H system (Metrohm) is used to collect the Raman spectra, with 100% laser power with a 20 s integration time and averaged three times. In one instance, the timeline plugin together with digital input/output (DIO) triggering from the AUT204 is used to collect Raman spectra while stepping the voltage in a chronoamperometry (CA) experiment.

**Table 2.** Parameters used in electrochemical roughening

Component	Part 3
Technique	Chronoamperometry (CA), linear sweep voltammetry (LSV)
Parameters	Repeat 25x, -0.3 V (CA, 30s) -0.3 to 1.2 V, 10 mV/s (LSV) 1.2 V (CA, 60s) 1.2 to -0.3 V, 10 mV/s (LSV)
Cell	DRP-RAMANCELL-M
Working electrode	QCM Au Crystal
Counter electrode	Pt wire
Reference electrode	Ag/AgCl
Electrolyte	0.1 mol/L KCl

## RESULTS AND DISCUSSIONS

### Part 1 – Deposition experiment

Figure 2 displays the electrochemical and synchronized QCM-D data. The potential (green) drops rapidly before reaching a steady state, which is consistent with most chronopotentiometry experiments. The corresponding drop in the QCM (grey) and small changes in the damping signal (orange) data are shown.

It is expected that the deposited nickel hydroxide layer is rigid, which is confirmed by the insignificant damping (<10% of the frequency shift). This means the Sauerbrey model can be applied with a high degree of confidence about its accuracy [2]. For less rigid layers, viscoelastic modelling provides a better accuracy for data interpretation. Analysis based on either option are available in the qGraph Viewer software.

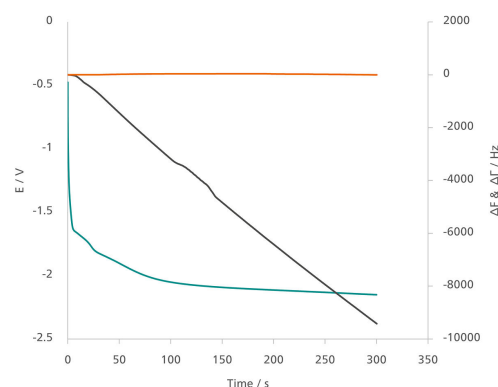


**Figure 2.** Synchronized potential (E vs time, green), resonance frequency (grey) and damping (orange) signals recorded during the course of the deposition.

The deposition is accompanied by a change in resonance frequency of about -9500 Hz. Using the Sauerbrey Equation (below), this corresponds to about 41,000 ng/cm<sup>2</sup> loaded on to the crystal.

$$\Delta \phi = -C_f \cdot \Delta f$$

The damping signal (**Figure 3**) provides useful information about the surface topography. For viscoelastic layers, e.g., polymers, damping is generally the result of dissipative energy losses due to deformation of the adsorbed material. For rigid layers analyzed in this study, however, the mechanism is quite different. Here, damping or dissipation comes from hydrodynamic interactions between the rough surface and the surrounding electrolyte [2].

A rougher or more porous surface leads to a larger interaction and therefore a larger change in the damping signal. For a rigid layer, there are only a handful of scenarios that can occur as the deposition progresses:

1. The damping signal simply increases constantly, this occurs when the layer is thick, rough, and dendrites are also forming.
2. The damping signal rises but reaches a maximum, corresponding to a less rough surface without dendrites.
3. The signal initially rises and then falls back to zero, corresponding to a simple flat rigid layer [2].

**Figure 3** clearly shows the final scenario occurs during this experiment. The damping signal initially rises as islands (of Ni(OH)<sub>2</sub>) will form on the electrode at the start of deposition, which creates an artificial roughness, allowing for the

Where  $C_f = 4.3 \text{ ng cm}^{-2} \text{ Hz}^{-1}$  is the sensitivity coefficient for this crystal, and  $\Delta \phi = \Delta m / A_q$  represents the area density. The layer thickness can then be calculated by dividing  $\Delta \phi$  by the material density  $\rho$ .

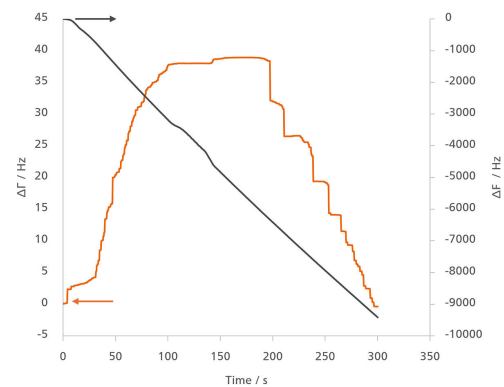


**Figure 3.** Close up view of the damping signal (orange) (fundamental frequency, F1), recorded during the electrochemical deposition. In grey the resonance frequency is shown.

needed hydrodynamic interactions to occur. As the deposition continues, the islands eventually transition to a 'complete' layer, the interactions disappear, and the damping signal returns to zero.

## Part 2 – Cyclic voltammetry experiment

The deposited layer can be cycled, according to:



This reaction is the basis for cathode reaction in Ni-MH batteries. Cycling produces measurable mass change in the  $\text{Ni(OH)}_2$  layer as the hydroxide is oxidized to the oxyhydroxide and back. During oxidation–reduction cycling, approximately 1500 ng/cm<sup>2</sup> is reversibly added

It is simple to associate the electrochemical data with the QCM data using tools available in the qGraph Viewer software, allowing for easy synchronization between both signals. This is shown in **Figure 4**. Under the few numbers of sweeps conducted the mass signal changes (as well as the electrochemical signal) are reversible. However, changes in the mass or damping signal as a result of cycling can be an early indicator of side reactions, as well as a powerful aid in studying electrode deformations and mechanically characterizing electrodes in-situ [5,6].

## Part 3 – EC-Raman

In **Figure 5**, the EC-Raman cell used in this part of the experiment is shown. It is mounted in position on the Raman probe holder.

or removed, corresponding to a  $\pm 3$  nm change in layer thickness. This is largely due to the intercalation of water and electrolyte cations in the structure during the cycling. In this case both the damping and frequency signals also returns to almost zero, indicating this is a largely reversible process [4].

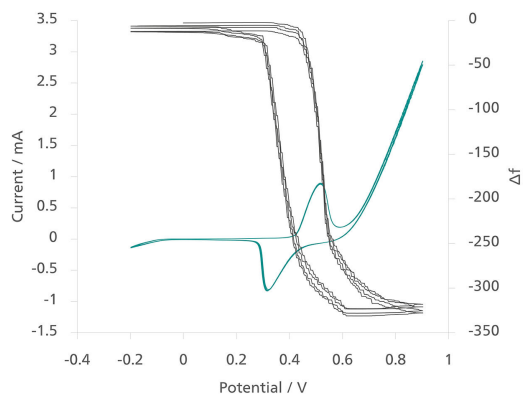


**Figure 4.** Synchronized CV (green) and EQCM (grey) signals.

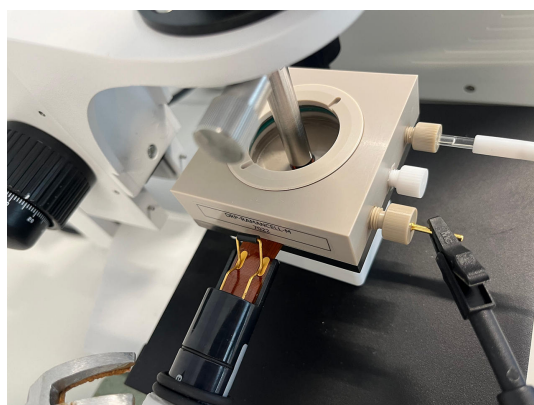


**Figure 5.** EC-Raman cell with the Raman probe and probe holder in the center. At the sides of the cell are the electrodes and the EQCM-D probe visible.

After roughening the SERS substrate, a layer of  $\text{Ni}(\text{OH})_2$  is deposited, which according to the EQCM data has roughly the same thickness as in part 1. The layer is then cycled by applying appropriate potential for 30 s to sufficiently oxidize it to  $\text{NiOOH}$  (0.65 V) or reduce it to  $\text{Ni}(\text{OH})_2$  (-0.2 V). Raman spectra are collected at each potential and are shown in **Figure 6**. While  $\text{Ni}(\text{OH})_2$  appears to be Raman inactive in the 200–800  $\text{cm}^{-1}$  region,  $\text{NiOOH}$  has two peaks at 476 and 556  $\text{cm}^{-1}$ . Chronoamperometry EC-Raman in four, 30-second steps at -0.2, 0, 0.3 and 0.6 V is also conducted proving the transformation.

## CONCLUSION

A system for EQCM-D is presented, consisting of a Metrohm Autolab AUT204 and a 3T analytik eSorptionProbe OS. The system is versatile and easy to handle, with the probe being insertable into a variety of different cells, and the electrode being compatible with a range of chemicals. In this Application Note, the system is successfully applied to the deposition and subsequent electrochemical cycling of nickel hydroxide,

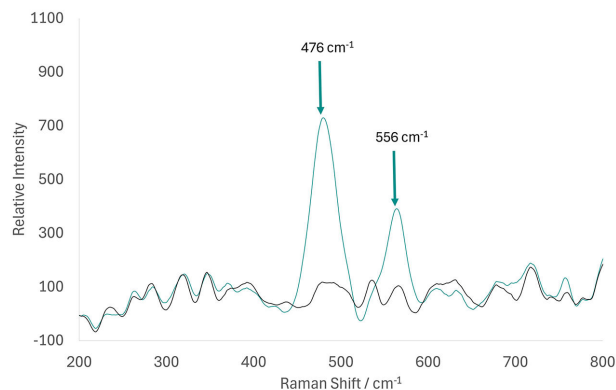


**Figure 6.** EC Raman, conducted at -0.2 V (grey) and 0.65 V (green) corresponding to electrochemical cycling of  $\text{Ni}(\text{OH})_2$  into  $\text{NiOOH}$ .

demonstrating its usefulness for battery applications.

The versatility and power of the EQCM-D probe system is further proven by integrating it into an EC-Raman cell. Opening new avenues for research using the system, with an in-situ monitoring of both a Raman and EQCM signal being a very powerful option.

## REFERENCES

1. Ortner, P.; Umlandt, M.; Lomadze, N.; et al. Artifact Correction of Light Induced Detuning in QCM-D Experiments. *Anal. Chem.* **2023**, *95* (42), 15645–15655. <https://doi.org/10.1021/acs.analchem.3c02814>.
2. Vanoppen, V.; Johannsmann, D.; Hou, X.; et al. Exploring Metal Electroplating for Energy Storage by Quartz Crystal Microbalance: A Review. *Advanced Sensor Research* **2024**, *3* (9), 2400025. <https://doi.org/10.1002/adsr.202400025>.
3. Realizing Two-Electron Transfer in Ni(OH)<sub>2</sub> Nanosheets for Energy Storage | *Journal of the American Chemical Society*. <https://pubs.acs.org/doi/10.1021/jacs.1c13523> (accessed 2025-08-19).
4. Wu, T.-H.; Scivetti, I.; Chen, J.-C.; et al. Quantitative Resolution of Complex Stoichiometric Changes during Electrochemical Cycling by Density Functional Theory-Assisted Electrochemical Quartz Crystal Microbalance. *ACS Appl. Energy Mater.* **2020**, *3* (4), 3347–3357. <https://doi.org/10.1021/acsaem.9b02386>.
5. Levi, M. D.; Daikhin, L.; Aurbach, D.; et al. Quartz Crystal Microbalance with Dissipation Monitoring (EQCM-D) for in-Situ Studies of Electrodes for Supercapacitors and Batteries: A Mini-Review. *Electrochemistry Communications* **2016**, *67*, 16–21. <https://doi.org/10.1016/j.elecom.2016.03.006>.
6. Shpigel, N.; Levi, M. D.; Aurbach, D. EQCM-D Technique for Complex Mechanical Characterization of Energy Storage Electrodes: Background and Practical Guide. *Energy Storage Materials* **2019**, *21*, 399–413. <https://doi.org/10.1016/j.ensm.2019.05.026>.

## CONTACT

瑞士万通中国  
北京市海淀区上地路1号院  
1号楼7702  
100085 北京

marketing@metrohm.com.cn

## CONFIGURATION



### Autolab PGSTAT204

PGSTAT204 合了小巧格和模化。器包括基本恒位/恒流,其从 20 V,最大流 400 mA 或 10 A,与 BOOSTER10A 合使用。此恒位可随用附加模行展,例如 FRA32M 化学阻抗(EIS)模。

PGSTAT204 是一款惠的器,可置于室的任何位置。具有模和数字入/出,可控制 Autolab 附件和外部。PGSTAT204 包括内置模分器。与高性能的 NOVA 件用,可用于大多数准化学技。